Jan 15th, 11:45 AM - 12:00 PM

Improving the Wave Forecasting in the Catalan Coast (WAM Cycle 4.5)

Adria Moya
Universitat Politècnica de Catalunya (UPC). Barcelona, Spain, adriamoyaortiz@gmail.com

Agustín Sánchez-Arcilla
Laboratori d'Enginyeria Marítima (LIM/UPC), Universitat Politècnica de Catalunya (UPC). Barcelona, Spain

Gerbrant Ph. Van Vledder
Delft University of Technology, Civil Engineering and Geosciences Department, Delft, The Netherlands

Improving the Wave Forecasting in the Catalan Coast (WAM Cycle 4.5)

Adrià Moya[1,2)*], Agustín Sánchez-Arcilla[3,4)], Jesús Gómez[3,4)] and Gerbrant Ph. Van Vledder[2)]
[1)] Universitat Politècnica de Catalunya (UPC). Barcelona, Spain
[2)] Delft University of Technology, Civil Engineering and Geosciences Department, Delft, The Netherlands
[3)] Laboratori d'Enginyeria Marítima (LIM/UPC), Universitat Politècnica de Catalunya (UPC). Barcelona, Spain
[4)] Centre Internacional d'Investigació dels Recursos Costaners (CIIRC), Barcelona, Spain
[*]Corresponding author: adriamoyaortiz@gmail.com

Abstract—The present study investigates the conspicuous shortcomings of the whitecapping dissipation model implemented in WAM Cycle 4.5 [1], following the lead of the work of [2] and [3]. Its dependence on an overall wave steepness unavoidably yields systematic errors when more than one wave system is propagating. The complex orography and highly variable winds at the Catalan coast lead to fetch- and duration-limited wave conditions near the Ebro delta. The incidence of swell trains during the development of these wind-seas coming from land favors the development of bimodal spectra. Although a comprehensive tuning of the free parameters of the dissipation function is performed, effectively improving the general subestimation of wave periods, it is strongly recommended to incorporate updated dissipation models, which avoid the dependence on an overall wave steepness and provide a more physical description of the wave breaking mechanism[4]; [5].

1. Introduction

This work was mainly originated with the goal of improving the current wave forecasting situation at the Catalan coast. It is known that the "Servei Meteorològic de Catalunya" (SMC), also known as "Meteocat", has driven its wave forecasts by using the wave model WAM over the Western Mediterranean Sea. Therefore, this study will be principally focused on getting deep insight into the wave model and, secondly, seeking the reasons by which non-negligible divergence exists between the outputs of such a model and the real measurements.

The main purpose of this study, therefore, is to investigate the effect of whitecapping dissipation on the temporal evolution of the wave spectrum, identify the causes that lead to significant errors and propose a suitable calibration of the tunable parameters of this least understood part of the physics, supported on comprehensive spectral and integral analyses. Such modifications attempt to correct, or at least improve, the frequent disagreement between predicted and observed wave data at the Catalan coast, especially during storm conditions. Particular attention is drawn to the Ebro delta area, not only because of the growing need to properly track its evolution but due to the common presence of characteristic bimodal spectra, caused by the coexistence of wind-seas and swells.

2. Physics

2.1. Energy balance equation

The evolution of the energy density $E(f,\theta)$ of each wave component can be obtained by integrating an energy balance equation while propagating with the group velocity along a wave ray:

$$\frac{\mathrm{d}E(f,\theta;x,y,t)}{\mathrm{d}t} = S(f,\theta;x,y,t) \quad (1)$$

where the term on the left-hand side is the rate of change of the energy density, and $\mathrm{d}x/\mathrm{d}t = c_{g,x}$ and $\mathrm{d}y/\mathrm{d}t = c_{g,y}$ (where $c_{g,x}$ and $c_{g,y}$ are the x- and y-components of the group velocity of the wave component under consideration), and frequency and direction are constant (in deep water). The term on the right-hand side (called the source term) represents all effects of generation, wave–wave interactions and dissipation. Developing the Eq. (1):

$$\frac{\partial E(f,\theta)}{\partial t} + \frac{\partial c_{g,x}E(f,\theta)}{\partial x} + \frac{\partial c_{g,y}E(f,\theta)}{\partial y} = S(f,\theta) \quad (2)$$

The source term $S_{tot} = S(f,\theta)$ is often written as:

$$S_{tot} = S_{in} + S_{nl4} + S_{ds} \quad (3)$$

These terms denote, respectively, wave growth by the wind, nonlinear transfer of wave energy through four-wave interactions and wave decay due to whitecapping wave breaking in deep water.

2.2. Source terms

The wind input formulation was adopted by [6] and the transfer of wind energy to the waves is described with a resonance mechanism [7] and a feed-back mechanism [8]:

$$S_{in} = \alpha + \beta E(f,\theta) \quad (4)$$

in which α describes the linear growth and $\beta E(f,\theta)$ exponential growth. For the WAM Cycle 4.5, although the model is driven by the wind speed at 10 m elevation U_{10}, it uses the friction velocity u_*. The computation of u_* is an integral part of the source term and it represents an alternative measure

for stress or momentum flux.

The second mechanism that affects wave growth in deep water is the transfer of energy among the waves, i.e., from one wave component to another, by resonance. The numerical implementation of the quadruplet wave-wave interactions is achieved with the development of the Discrete Interaction Approximation (DIA) as proposed by [9], which proved sufficiently economical for application in operational wave models.

Wave breaking in deep water (whitecapping) is a very complicated phenomenon, which so far has defied theoretical understanding. Generally, there is no accepted, precise definition of breaking and, additionally, quantitative observations are very difficult to carry out. Due to this reason, it is common practice to calibrate numerical wave models by tuning the parameters included in the corresponding formulation. In the present cycle of the WAM model, the process of whitecapping is represented by the pressure pulse-based model of [10], reformulated in terms of the wave number (rather than frequency), so as to be applicable in finite water depth (cf. [1]). This expression is:

$$S_{ds} = -C_{ds}\left[(1-\delta) + \delta\frac{k}{\langle k\rangle}\right]\left(\frac{\hat{s}}{\hat{s}_{PM}}\right)^{p}\frac{k}{\langle k\rangle}E(f,\theta) \qquad (5)$$

The coefficients C_{ds}, δ and p are tunable coefficients, $\hat{s}$ is the overall wave steepness, $\hat{s}_{PM}$ is the value of $\hat{s}$ for the Pierson- Moskowitz spectrum [11], and it is equal to $\hat{s}_{PM} = \sqrt{3.02 \times 10^{-3}}$. The values of the tunable coefficients in this model were obtained by [12] by closing the energy balance of the waves in idealized wave growth conditions (both for growing and fully developed wind-seas) for deep water. This implies that coefficients depend on the wind input formulation that is used. For the wind input of [13] and [14] it was obtained (assuming $p = 2$) $C_{ds} = 4.10 \times 10^{-5}$ and $\delta = 0.5$ (as used in the WAM Cycle 4; [14]). The theory on which the WAM model is based is described in more detail in [1].

3. The Catalan coast

The Mediterranean Sea is a semi-enclosed sea for it has limited exchange of water with the outer ocean. For practical reasons, it can be considered as a big lake in the sense that it is highly influenced by the coastline and the surrounding orography. Wave forecasting in this region is subject of extensive research and important progress has been achieved so far.

The reasons for the limited predictability in the study region are determined by a wave climate controlled by (1) short fetches, (2) shadow effect of waves from the south and east due to the Balearic islands, (3) complex bathymetry with deep canyons close to the coast, (4) high wind field variability in the time and space, (5) wave calms during the summer and energetic storms from October to May (marked seasonality), (6) presence of wind jets canalized by river valleys, (7) sea and swell waves combination that generate bimodal spectra and (8) relatively short periods associated with swell waves, which compromise the proper distinction between wind-sea and swell.

The abovementioned factors yield a characteristic behavior of integral parameters during storm conditions. More specifically, underestimation of wave height maximum values and overestimation of wave heights during calm periods is often observed [15]. Additionally, wave periods still suffer a notable underprediction. Pallares et al. [3], however, obtained a clear improvement of the mean wave period and the peak period at the Catalan coast, decreasing considerably the negative bias observed. Nevertheless, almost no change was observed in wave height due to the proposed modification.

Rogers et al. [2] observed a similar underprediction pattern and concluded that the cause lied in an underprediction of low- and medium-frequency energy in the modeled spectrum, together with an overly strong dissipation of the swell.

4. Model set-up

The WAM Cycle 4.5.3 [1] is run in two nested grids covering all the Northwestern Mediterranean Sea with a grid resolution from 9 to 3 km (Table 1), forced with corresponding low and high-resolution six-hourly wind fields (WRF), for two typical storm events during January 2010.

Table 1. Computational grids implemented in the wave model run for both Balearic (BS) and Western Mediterranean Sea (WM).

	Western Mediterranean Sea (WM)	**Balearic Sea (BS)**
Longitudes	4.95°W - 16.00°E	0.45°W - 5.58°E
Latitudes	35.10°N - 44.62°N	39.00°N - 43.66°N
Mesh size	196×119	168×173
Grid resolution	9 km (0.107°×0.081°)	3 km (0.036°×0.027°)

The frequency range considered is chosen according with the buoy frequency domain, which is 0.030–0.625 Hz, resulting in 33 frequency values that

range from 0.03 Hz to 0.633 Hz.

Additionally, the model runs are computed using a cold start. It has been observed, however, that the generation of wave forcing at the southern boundary of the coarse grid (WM), between the longitudes 10°E and 12°E, led no changes in the estimations at the three buoy stations. Note that this is only implemented at the very first step of the computation run; every new step assumes that the initial sea state is equal to the previous time step.

During the study interval (from Jan 6th to Jan 18th, 2010), waves were monitored by several wave-measuring instruments although the study presented herein uses three main buoys (Tortosa, Llobregat and Blanes; see Fig. 1). Directional Waverider buoys provide direct pitch-and-roll wave measurements. Identification of different wave systems is accomplished through reconstruction of buoys' two-dimensional spectra and further application of spectral partitioning techniques.

From this study interval, two storm events can be recognized based upon a reasonable threshold of 1.5 m of significant wave height (SWH) during more than 6 h [15]. The parameters considered for validation are:

SWH	H_{m0}	$H_{m0} = 4\sqrt{m_0}$
Mean-zero crossing period	T_{m02}	$T_{m02} = \sqrt{\frac{m_0}{m_2}}$
Peak period	T_p	$T_p = 1/f_p$
Mean wave direction	θ_m	$\theta_m = \tan^{-1}\left[\frac{\int \sin\theta\, E(f,\theta)\mathrm{d}f\mathrm{d}\theta}{\int \cos\theta\, E(f,\theta)\mathrm{d}f\mathrm{d}\theta}\right]$

5. Analysis of the results

5.1. First storm event (Jan 7th to Jan 12th, 2010)

This first storm is characterized by the dominance of two different sea states. First, wind coming from the east may correspond to air fluxes from the low pressure center over the sea. It is in this direction where developed wave conditions (associated with swell wave groups) may occur. On the other hand, wind coming from the northwest (at Tortosa) corresponds to air flow channeled by the Ebro river valley and blows towards the sea through the opening in the coastal mountain chain. The latter characteristic offshore-blowing winds result in fetch- and duration-limited growth conditions that commonly produce wind-sea waves at Tortosa.

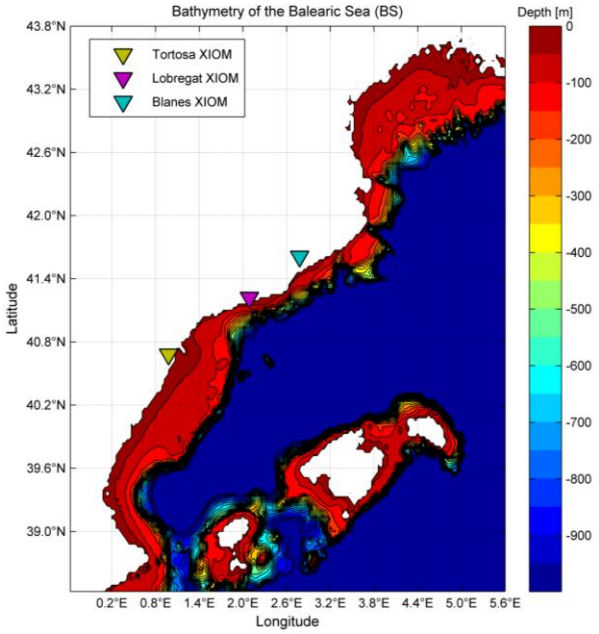

Figure 1. Bathymetry of the Balearic Sea (BS).

Swell waves are recorded during the peak of the storm (Jan 8th, at 00:00 h), whereas the second part of the storm, when swell dissipates, is determined by the mentioned wind-seas (see Fig. 2).

The energy content associated with the low-frequency peak is clearly underestimated regardless of the modifications proposed. Thereafter, it can be argued that there is an overly dissipation of energy by the time the storm reaches its peak (Jan 8th, at 00:00 h). Given the fact that wind-sea waves also grow during this first part of the storm, bimodal spectra are found at this location. The overall wave steepness, which largely affects the whitecapping dissipation model [Eq. (5)], increases, thus producing a higher energy dissipation rate. It can be seen, however, that the dissipation coefficient C'_{ds} significantly corrects this fictitious dissipation of low- frequency energy, when reduced to 0.5.

During the second part of the storm a better agreement is found. At this time, the energy spectrum widens and its peak shifts to higher frequencies due to the wind growth and progressive weakening of swell incidence. Here, a small dissipation coefficient yields too much energy (at all frequencies) and, hence, wave heights are slightly overestimated.

The mean wave period T_{m02}, on the other hand, is underestimated throughout the length of the storm (Fig. 3). It has been concluded that this is the result of

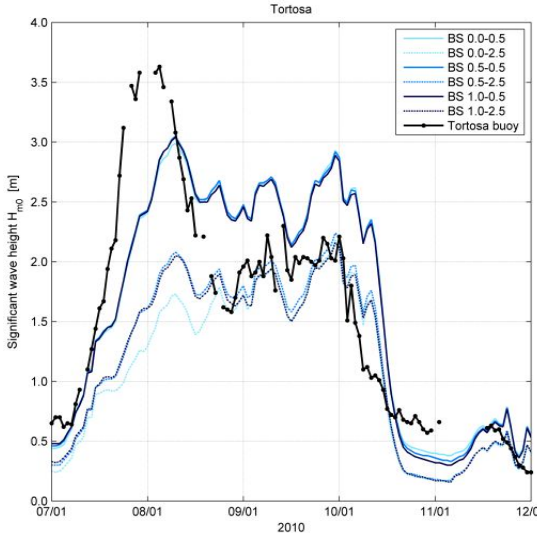

Figure 2. Comparison of temporal evolution of the significant wave height for different whitecapping coefficients at the buoy of Tortosa during the first storm event. Note that the combination of values stands for the delta and dissipation coefficient values ($\boldsymbol{\delta}$-$\boldsymbol{C'_{ds}}$).

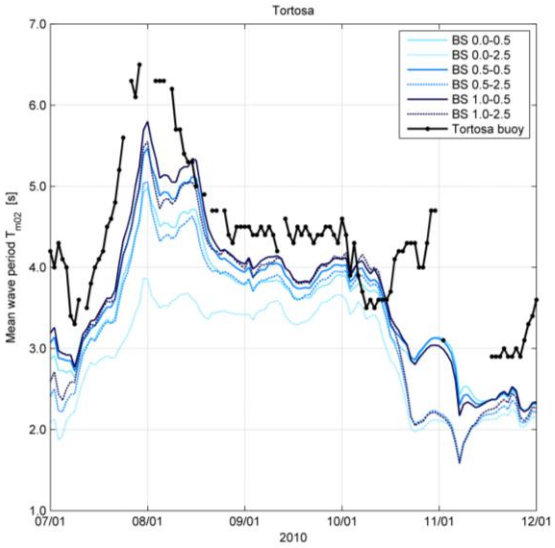

Figure 3. Comparison of temporal evolution of the mean (zero-crossing) wave period for different whitecapping coefficients at the buoy of Tortosa during the first storm event.

an overestimation of high-frequency energy in the wave spectrum. The physical description of the mean wave period is very sensitive to the amount of high-frequency energy due to the dependence on the second-order spectral moment m_{02}, which in turn is largely influenced by the square of the frequency. Therefore, the second-order spectral moment dramatically gives more weight to energy at high frequencies. Consequently, an overestimation of m_{02} leads to an underestimate of the mean wave period. Nevertheless, mean wave period can be substantially modulated and, most importantly, corrected by using a low dissipation coefficient and a large delta value ($\delta = 1$), thus enabling full dependence on the wave number [Eq.(5)].

Ultimately, mean wave directions are well reproduced by the model and only very small changes are induced by tuning the dissipation coefficients.

5.2. Second storm event (Jan 14th to Jan 16th, 2010)

The distinctive feature of the present storm event is the occurrence of a strong coastal wind jet off the coast at the Ebro delta. Even though presence of swell trains is reported during the beginning and end of such a storm, the most intense moments are driven by the high wind-energy input by part of the offshore-blowing wind associated with the coastal wind jet. In short, the main difference between this and the precedent storm is the sudden growth in wind speeds at Tortosa. Additionally, it can be seen that this strong wind event is locally generated and no large variations in wind velocity are reproduced in the two other

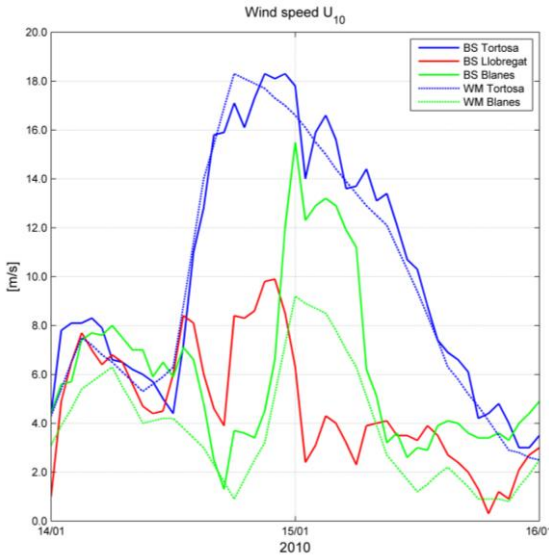

Figure 4. Temporal variation of computed wind velocities at the three different locations during the second storm event

locations (see Fig. 4), thus underscoring the consequential role played by orography.

Even though it could be stated that there is a general-

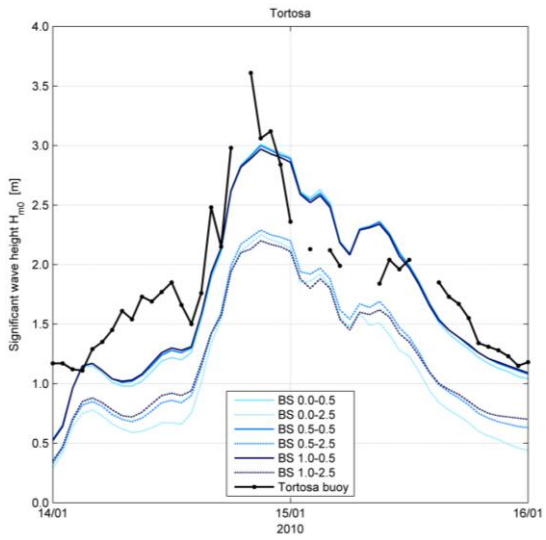

Figure 5. Comparison of temporal evolution of the significant wave height for different whitecapping coefficients at the buoy of Tortosa during the second storm event.

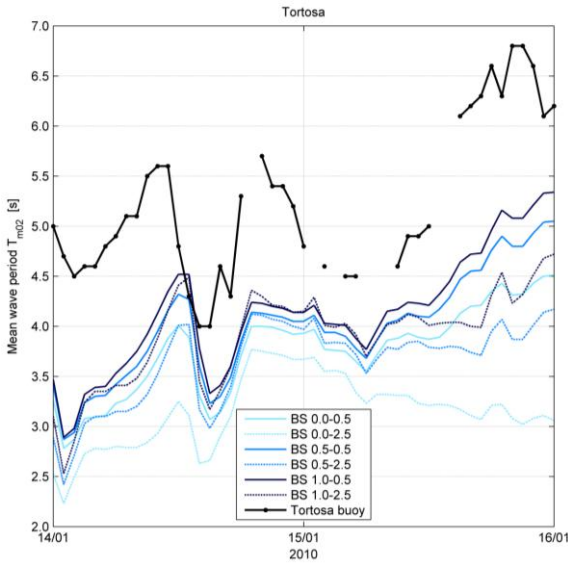

Figure 6. Comparison of temporal evolution of the mean (zero-crossing) wave period for different whitecapping coefficients at the buoy of Tortosa during the second storm event.

ized underprediction of wave periods and wave heights (not always true for the latter), better agreement between observed and estimated data exists in this second storm event. Despite the slight underestimation, significant wave heights are reasonably well predicted (for low-dissipation coefficients), although any of the proposed modifications captures the peak of the storm on Jan 14, at 21:00 h (see Fig. 5). The low-frequency energy (0.11-0.15 Hz), present during the first hours of the storm event, is clearly underpredicted, thus explaining the small wave heights at the beginning and agreeing with the fictitious dissipation of swell already found. Moving chronologically through the storm it can be seen that good agreement exists when it comes to low-dissipation coefficient combinations ($\boldsymbol{C'_{ds}} = \mathbf{0.5}$; the delta value hardly influences wave heights, in accordance with the previous storm).

The fact that an energy peak is generated right at the peak of the storm, over the whole frequency range, puts on record the high intensity and short duration of the coastal wind jet. However, given that it is not well-captured by the wave model, it suggests that this shortcoming lies in the fact that input wind fields have not correctly reproduced the sudden growth in speed.

The evolution of the mean and peak wave periods exposes the recurrent underprediction problem reported by many authors in semi-enclosed basins and bays. Therefore, both peak wave T_p and mean periods T_{m02} display differences of more than 1 s on average. However, in accordance with the analysis of the previous storm, the (1.0-0.5) combination provides best fitting (see Fig. 6). The existence of large scatter suggests that wave periods are strongly influenced by these two parameters (especially by the delta value, which balances the low- and high-frequency energy).

The last integral parameter reviewed is the mean wave direction (see Fig. 7), which is fairly well estimated; in particular wave groups coming from the south (Jan 14, between 00:00 and 15:00 h) and, later, associated with directions coming from the northwest (between the Jan 14, at 15:00 h and Jan 15, at 09:00 h).

6. Discussion

6.1. Impact on spectral energy

So far, underestimation of low-frequency energy has become a systematic error. Rogers et al. [2] suggested that underprediction of low-frequency energy can be attributed to one or more of the three deep-water source/sink terms and, focusing in the spectral dissipation, affirmed that can be also related to bulk parameters (e.g., mean steepness) that are influenced by the overly prediction of high-frequency energy.

Rogers et al. [2] reported successful results tuning the exponential coefficient $\boldsymbol{p}$ to 2 in the whitecap model [Eq. (5)], leading to an increase of energy at low fre-

quencies and decreasing high-frequency energy. This is due to the fact that the exponential coefficient acts on the wave steepness and, therefore, larger steepness associated with high-frequency waves will lead to larger dissipation, thus decreasing energy at that frequency range. In the present report it was not attempted to tune this third coefficient and, following the lead of [2], it was left by default at 2. A strong

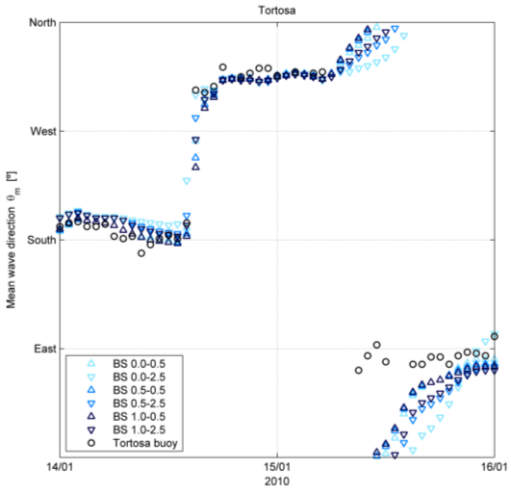

Figure 7. Comparison of temporal evolution of the mean wave direction for different whitecapping coefficients at the buoy of Tortosa during the second storm event.

focus has been placed, however, on tuning the two remaining parameters ($\boldsymbol{C'_{ds}}$ and $\boldsymbol{\delta}$).

The wave model (WAM Cy 4.5.3) dissipation source function was reformulated in terms of a mean wave steepness and a mean frequency in order to give more emphasis on the high-frequency part of the spectrum (based on [10]'s analytical model for whitecap dissipation according to [12]). Unfortunately, all tests by [12] were performed for wind-sea growth in the absence of swell, which was later found to generate problems inherent to the definition of a mean steepness from the entire spectrum, leading to overestimations of wind-sea growth in the presence of swell, even with the latest modification to [12]'s formulation by [16].

This shortcoming can be clearly seen during the low-frequency energy dominant peak generated at the beginning of the first storm event, in presence of a wind-energy input at higher frequencies or, similarly, when the wind-wave growth develops during the dissipation of the eastern swell in the same storm. Bimodality exists in both situations although a dominant wave group can be discerned in each one. Even though one might need to carefully examine it, low-frequency energy is always underestimated (below 0.10 Hz) and high-frequency energy is overestimated most of the time, especially when wind-sea energy is dominant (above 0.30 Hz). The latter overestimation might not be only induced due to low dissipation (resulting from mean wave steepness) but the approximation of the spectral tail, which seems to substantially yield too much energy at high frequencies.

6.2. Impact on integral parameters

Different impact on integral parameters is driven by each coefficient. Significant wave heights are largely influenced by the dissipation coefficient C'_{ds}, which in turn has lower effect on wave periods. This is due to the fact that whitecapping dissipation has linear dependence on this coefficient [Eq.(5)] and, therefore, if reduced, lower dissipation is guaranteed for the whole frequency range, leading to a larger overall amount of spectral energy and, hence, larger wave heights. The delta value, on the other hand, modulates the dependency on the wave number (i.e., the length of the waves) and its contribution is more subtle.

When the delta coefficient is raised to 1, maximum dependence on wave number is assured, thus yielding more dissipation at high-frequencies (short wave lengths) and lower at low-frequencies (long wave lengths). Due to the latter statement, better agreement is provided when delta is raised, thus coping with the negative adverse effect introduced by the dependence on the mean wave steepness. In addition, when implementing this modification, whitecapping dissipation places more weight on the high-frequency range and, as a result, the second-order spectral moment reduces because of the lower energy content at high frequencies. This outcome results in a substantial enhancement in the mean wave period T_{m02}, thus improving the well-known tendency to underpredict this parameter in the Catalan coast.

6.3. Statistical analysis

Even though statistical parameters are representative when long time series are available (two or three months, at least), they give a quantitative evaluation of the degree of accuracy of simulation results and will serve to support the results of the spectral analysis. The main statistical parameters are the root mean square error (RMSE), the bias, the scatter index (SI), the correlation coefficient (R) and the mean absolute error (MAE):

$$\text{RMSE} = \sqrt{\frac{1}{N}\sum_{i=1}^{n}(S_i - O_i)^2} \qquad (6)$$

Table 2. Summary of the statistical errors for the simulations during the first storm event.

	RMSE			**BIAS**			**SI**			**R**			**MAE**	
	WM	**BS**		**WM**	**BS**		**WM**	**BS**		**WM**	**BS**		**WM**	**BS**
1.0-0.5														
H_{m0}	**0.531 m**	**0.580 m**		-0.071 m	**0.162 m**		**0.337**	**0.368**		**0.805**	**0.811**			
T_p	2.465 s	**2.271 s**		**-1.201 s**	**-0.962 s**		0.369	**0.340**		0.471	**0.520**			
T_{m02}	**0.954 s**	**0.760 s**		**-0.790 s**	**-0.588 s**		**0.221**	**0.176**		0.776	**0.829**			
θ_m	100.756°	92.150°		26.151°	13.232°		0.501	**0.458**		0.666	**0.710**		43.565°	38.323°

Table 3. Summary of the statistical errors for the simulations during the second storm event.

	RMSE			**BIAS**			**SI**			**R**			**MAE**	
	WM	**BS**		**WM**	**BS**		**WM**	**BS**		**WM**	**BS**		**WM**	**BS**
1.0-0.5														
H_{m0}	**0.418 m**	**0.359 m**		-0.251 m	0.180 m		0.229	**0.196**		0.898	0.883			
T_p	**1.713 s**	**1.721 s**		**-1.261 s**	**-1.259 s**		**0.229**	**0.230**		**0.808**	**0.808**			
T_{m02}	**1.300 s**	1.196 s		**-0.790 s**	**-1.098 s**		**0.248**	**0.228**		**0.783**	**0.791**			
θ_m	75.337°	64.260°		15.414°	2.756°		0.399	0.340		0.725	0.784		17.951°	17.146°

$$\text{bias} = \frac{1}{N}\sum_{i=1}^{n}(S_i - O_i) \tag{7}$$

$$\text{SI} = \frac{RMSE}{{}^{1}/_{N}\sum_{i=1}^{n} O_i} \tag{8}$$

$$\text{R} = \frac{\sum_{i=1}^{n}\{(S_i - \langle S\rangle)(O_i - \langle O\rangle)\}}{\sqrt{\{\sum_{i=1}^{n}(S_i - \langle S\rangle)^2\}\{\sum_{i=1}^{n}(O_i - \langle O\rangle)^2\}}} \tag{9}$$

$$\text{MAE} = \frac{\sum_{i=1}^{n}\Delta\theta_{O,S}}{N} \tag{10}$$

where O_i is the observed value, $\langle O\rangle$ is the mean value of the observed data, S_i is the simulated value, $\langle S\rangle$is the mean value of the simulated data and N is the number of data. The shortest distance $\Delta\theta_{1,2}$ between two directions is computed as: $\Delta\theta_{1,2} = 180 - \left|180 - |\theta_1 - \theta_2|\right|$.

Table 2 and Table 3 display the above mentioned statistical parameters for the chosen combination (1-0.5) of whitecapping coefficients and integral parameters.

Significant wave heights show higher correlation in general, although there is no clear trend with respect to positive or negative bias. This, however, is completely true for wave periods. Negative bias in both mean and peak wave periods is observed in both storm events, regardless of the combination proposed. A result of value is displayed by the very low correlation coefficient exhibited by the peak period during the first storm (characterized by bimodal spectrum). Similar bias is found in peak periods during both storms; however, in the first event larger scatter and root mean square errors are displayed. Another outcome that agrees with visual analysis is the fact that larger errors are encountered in mean wave directions during the first storm, in which different wave systems are found propagating in different directions at the same time.

It is also of interest to compare the results computed at different scales (i.e., different computational grids). Better agreement is found in virtually every parameter belonging to the high-resolution domain (BS), in relation with the coarse domain (WM). It is perhaps more interesting to note that some parameters provide better results when using data coming from the coarse grid (e.g., the scatter index SI for wave heights during the first storm; not shown here). Scatter indexes are expected to be lower with high-resolution data due to the enhanced accuracy (see Fig. 8).

Bertotti and Cavaleri [17] obtained systematically higher scatter in their small scale model and suggested that although ironically, this fact represents the capability of the high-resolution simulations (small scale) to go into higher details of the fields. However, the capability of reproducing realistic details does not imply these details are correct. Given a certain level of scatter between the actual data and a relatively smooth (lower resolution) field, the introduction of higher resolution details, physically consistent but not necessarily coincident with the real ones, leads una-

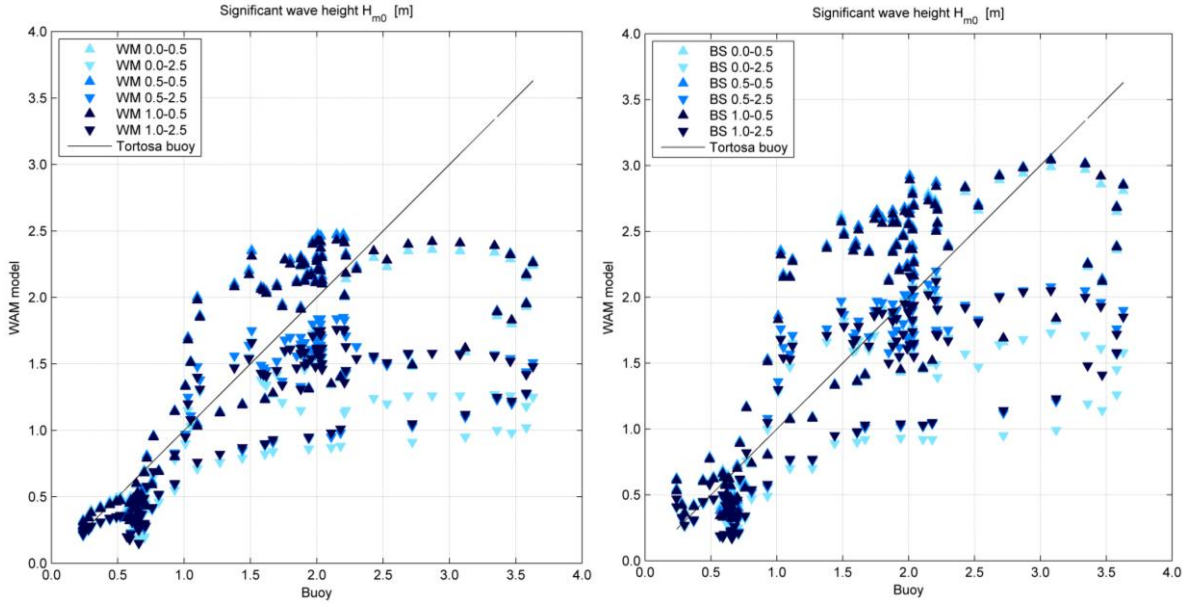

(a) Large-scale simulation (WM) (b) Small-scale simulation (BS)

Figure 8. Scatter plots for H_{m0} showing the larger scatter of the high-resolution simulation (BS). Results for the first storm event at Tortosa buoy.

voidably to a larger scatter (commonly referred as "double penalty").

Therefore, nested models, although capable of exceptional performances, cannot overcome all deficiencies. They simply focus on the details of a given area and, relying on their upper domain, do it correctly when correct information is provided [17].

6.4. Temporal and spatial resolution of wind fields

Furthermore, although not thoroughly explored in this research, it has been seen that the lack of temporal resolution in the wind fields can lead to not only underestimation, but even omission of the peaks and troughs of the temporal variations of significant wave height and average wave period. As an example, the large underestimation of the wind-sea peak (0.14-0.15 Hz) associated to the peak of the second storm (Jan 14, at 21:00 h): observed data suggest the existence of a coastal wind jet, the time scale of which was shorter than 6 h; thus pinpointing the too coarse temporal resolution of the wind fields implemented (6 h). Consequently, an increase of the temporal resolution is strongly recommended to properly capture the instantaneous effects of coastal wind jets at the buoy of Tortosa. On the other hand, it can be seen that the spatial resolution of the wind field is not as influential as the temporal at Tortosa. This can be concluded due to the fact that wind speed and directions are fairly similar in both fine (BS) and coarse (WM) grids (Fig. 4). However, in the same figure, important disagreement is found for the buoy of Blanes (and it is suspected that it would similarly occur at Llobregat). Alomar [18] reported the benefits of increasing wind variability in wave forecasting by increasing both the temporal and spatial resolution of the forcing wind fields. High resolution input winds prevent information losses in short-duration storm, especially in basins where the orography plays a substantial role.

7. Conclusions

The present (whitecapping) dissipation model [12] produces inconsistent results, especially marked differences with observed data during storm events. Although one cannot forget the important role played by the wind and nonlinear wave-wave interaction functions, it should be noted that dissipation of energy largely influences the energy balance and, hence, derived spectral parameters.

It has been found a low-frequency energy underestimation and high-frequency energy overestimation in the wave spectrum. This outcome was confirmed due to the overall steepness dependence of the dissipation model of [12]. The numerical implementation of the diagnostic tail might enhance this undesired effect. As a result, due to the different distribution of energy density, spectral moments will unavoidably change and, hence, spectral parameters such as H_{m0}, T_{m02} or T_p, will change as well. Therefore, an underestimation of wave periods occurs due to the over esti-

mation of high-frequency energy, whereas wave heights show no clear trend.

A low dissipation coefficient (C'_{ds}) and a delta value equal to 1 [Eq. (5)] yield a better agreement with observations. The fully dependence on wave number provided by this delta value compensates the spectral energy distribution explained in the second point, thus leading to slightly more energy at low frequencies and reducing the content at high frequencies [2], [3].

Evolution of coastal wind jets (as a result of the complex orography of the littoral) occurs at relatively short time scales (less than 6 h). Some observed peaks (e.g., H_{m0}) are missing in simulations. This is due to the fact that the time interval between consecutive wind fields is too large (6 h) and, therefore, wind-induced features occurring at time scales shorter than 6 h are not captured and reproduced by the model.

Nesting a computational grid (similarly for winds' mesh) with higher spatial resolution brings about more detailed results, which in most of the cases leads to better agreement with observed parameters.

8. Recommendations

Although it is argued that the present whitecapping formulation [12] produces inconsistent rates of energy dissipation, more satisfactory results (in storm conditions) can be obtained by keeping a low value for the dissipation coefficient, C'_{ds}, and setting the delta value, δ, equal to 1 (with the remaining tunable coefficient p equal to 2; [2].

Implement newer formulation for the dissipation source term [19] Recent formulation proposed by [4] and [5] offer better prospects for progress, although not fully tested. Therefore, for practical purposes, since WAVEWATCH III already incorporates [19]'s dissipation model, validation tests could be performed in order to evaluate the implementation of an updated formulation.

Prior to a calibration of wave growth rates and implementation of new source functions (if performed in future work), wind fields should be completely validated. Large sources of error generally come from wind fields rather than a not suitable description of the source terms.

Replacement of current six-hourly wind fields, by higher temporal resolution winds (at least three-hourly) in order to capture local features, such as the typical coastal wind jets, observed at the Ebro delta.

9. Acknowledgement

I would like to heartily thank Prof. Agustín Sánchez-Arcilla, who offered assistance and encouraged me to take on this research. Jesús Gómez, who I would like to express my sincere gratitude for his role in obtaining experimental data and proposing technical solutions. I owe special gratitude to Dr. Gerbrant Ph. van Vledder, who has provided me precious suggestions and advice. Without his guidance and encouragement through the past year at TUDelft, this study would not have been possible to accomplish. My sincere thanks also go to Elena Pallarès, who has provided me with constructive suggestions.

10. References

[1] WAMDIG, "The WAM model - A third generation ocean wave prediction model," *Journal of Physical Oceanography*, vol. 18, pp. 1775-1810, 1988.

[2] W. Erick Rogers, Paul A. Hwang, and David W. Wang, "Investigation of Wave Growth and Decay in the SWAN Model: Three Regional-Scale Applications," *Journal of Physical Oceanography*, vol. 33, 2003.

[3] Elena Pallares, Agustín Sánchez-Arcilla, and Manuel Espino, "Wave energy balance in wave models (SWAN) for semi-enclosed domains-Application to Catalan coast," *Continental Shelf Research*, vol. 87, pp. 41-53, 2014.

[4] F. Ardhuin et al., "Semiempirical Dissipation Source Functions for Ocean Waves. Part I: Definition, Calibration, and Validation," *Journal of Physical Oceanography*, vol. 40, pp. 1917-1941, 2010.

[5] W. E. Rogers, A. V. Babanin, and D. W. Wang, "Observation-Consistent Input and Whitecapping Dissipation in a Model for Wind-Generated Surface Waves: Description and Simple Calculations," *Journal of Atmospheric and Oceanic Technology*, vol. 29, pp. 1329-1346, 2012.

[6] R L Snyder, F W Dobson, J A Elliott, and R B Long, "Array measurements of atmospheric pressure fluctuations above surface gravity waves," *Journal of Fluid Mechanics*, vol. 102, pp. 1-59, 1981.

[7] O M Phillips, "On the generation of waves by turbulent wind," *Journal of Fluid Mechanics*, vol. 2, pp. 417-445, 1957.

[8] J W Miles, "On the generation of surface waves by shear flows," *Journal of Fluid Mechanics*, vol. 3, pp. 185-204, 1957.

[9] S. Hasselmann, K. Hasselmann, J. H. Allender, and T. P. Barnett, "Computations and Parameterizations of the Nonlinear Energy Transfer in a Gravity-Wave Spectrum. Part II: Parameterizations of the Nonlinear Energy Transfer for Application in Wave Models," *Journal of Physical Oceanography*, vol. 15, pp. 1378-1391, 1985.

[10] Klaus Hasselmann, "On the spectral dissipation of ocean waves due to white capping," *Boundary-Layer Meteorology*, vol. 6, pp. 107-127, 1974.

[11] Willard J. Pierson and Lionel Moskowitz, "A proposed spectral form for fully developed wind seas based on the similarity theory of S. A. Kitaigorodskii," *Journal of Geophysical Research*, vol. 69, pp. 5181-5190, 1964.

[12] G. J. Komen, S. Hasselmann, and K. Hasselmann, "On the Existence of a Fully Developed Wind-Sea Spectrum," *Journal of Physical Oceanography*, vol. 14, pp. 1271-1283, 1984.

[13] Peter A. E. M. Janssen, "Quasi-linear theory of wind wave generation applied to wave forecasting," *Journal of Physical Oceanography*, vol. 21, pp. 1631-1642, 1991.

[14] Heinz Günther, Susanne Hasselmann, and P. A. E. M. Janssen, "Report No. 4. The WAM Model Cycle 4," Hamburg, 1992.

[15] Rodolfo Bolaños, *Tormentas de oleaje en el Mediterráneo: Física y Predicción*. Barcelona, Spain: Universitat Politècnica de Catalunya, 2004.

[16] Jean Bidlot, Saleh Abdalla, and Peter Janssen, "A revised formulation for ocean wave dissipation in CY25R1," 2005.

[17] L. Bertotti and L. Cavaleri, "Large and small scale wave forecast in the Mediterranean Sea," *Natural Hazards and Earth System Sciences*, vol. 9, pp. 779-788, 2009.

[18] Marta Alomar, *Improving wave forecasting in variable wind conditions. The effect of ressolution and growth rate for the Catalan coast.* Barcelona: Universitat Politècnica de Catalunya, 2012.

[19] Hendrik L. Tolman and Dmitry Chalikov, "Source Terms in a Third-Generation Wind Wave Model," *Journal of Physical Oceanography*, vol. 26, pp. 2497-2518, 1996.

[20] N. Booij, R. C. Ris, and L. H. Holthuijsen, "A third-generation wave model for coastal regions: 1. Model description and validation," *Journal of Geophysical Research*, vol. 104, pp. 7649-7666, 1999.